Journal of Materials Chemistry A

PAPER

View Article Online
View Journal | View Issue

Cite this: J. Mater. Chem. A, 2019, 7, 13249

In situ room-temperature fabrication of a covalent organic framework and its bonded fiber for solid-phase microextraction of polychlorinated biphenyls in aquatic products†

Jing-Xuan Guo, [abc] Hai-Long Qian, [abc] Xu Zhao, [abc] Cheng Yang [c] and Xiu-Ping Yan *[abcd]

Development of new coating materials for solid-phase microextraction (SPME) along with facile methods for the fabrication of their firm coatings on SPME fibers is urgently needed for sample preparation. Here we show room-temperature preparation of a novel covalent organic framework (COF) TFPB-BD from 1,3,5-tris-(4-formylphenyl)benzene (TFPB) and benzidine (BD), and *in situ* room-temperature fabrication of a TFPB-BD bonded fiber for SPME of polychlorinated biphenyls (PCBs). TFPB and BD were employed as monomers for *in situ* growth of a new COF TFPB-BD on an amino-functionalized stainless steel fiber at room temperature. The developed TFPB-BD bonded fiber was used to develop a new SPME method for GC/MS/MS determination of trace PCBs in aquatic products. The developed analytical method gives enhancement factors of 4471–7488 and detection limits of 0.07–0.35 ng L^{-1}. The precision (RSD) for six replicate determinations of 100 ng L^{-1} PCBs with a single fiber and the fiber-to-fiber reproducibility for three parallel prepared fibers was in the range of 3.8–8.8%, and 5.3–9.7%, respectively. The recoveries for spiked 1.0 μg kg^{-1} PCBs in aquatic products were 87.1–99.7%.

Received 19th March 2019
Accepted 30th April 2019

DOI: 10.1039/c9ta02974e

rsc.li/materials-a

Introduction

Polychlorinated biphenyls (PCBs), a class of toxic persistent organic pollutants, have been discontinued since the late 1970s. Even so, humans and animals are still being exposed to PCBs due to their excellent stability, high lipophilicity, and long-range transport *via* the food chain.[1,2] Monitoring PCBs in food samples is of great significance. However, direct analysis of PCBs is usually difficult because of the trace level of PCBs and the complexity of the food matrix. Therefore, an efficient simple pretreatment is urgent for the enrichment of PCBs with simultaneous separation of matrices prior to determination.

Solid-phase microextraction (SPME) has attracted increasing attention due to its advantages of preconcentration and analyte/matrix separation, convenience, solvent-free nature, and easy conjunction with chromatography.[3,4] SPME has been widely used in food,[5–8] environmental,[9–11] and biological[12–14] analysis. The fiber coating plays a key role in SPME. Traditional SPME fibers such as polyacrylate (PA),[15] poly(dimethylsiloxane)/divinylbenzene (PDMS/DVB),[16] and polydimethylsiloxane (PDMS)[17] are not always satisfactory for a variety of analytes. Increasing research studies have focused on the development of new coating materials. To date, various coatings, such as metal oxide nanoparticles,[18,19] graphene,[20] metal–organic frameworks (MOFs),[21–23] and polymeric ionic liquids,[24] have been applied for the SPME of PCBs.

Covalent organic frameworks (COFs) are a new class of porous organic materials, which are orderly linked by organic monomers.[25–27] COFs have received extensive attention due to their promising applications in diverse areas such as gas capture,[28,29] catalysis,[30–32] sensing,[33–35] adsorption,[36–38] and separation.[39–41] The unusual characteristics such as high surface area, good thermal and solvent stability, and availability of in-pore functionality and surface modification endow COFs with great potential as novel coatings for SPME. In recent years, a variety of COFs have been utilized as SPME coatings.[42–49] Most of the COF coatings for SPME were prepared using physical adhesive methods,[42–47] suffering insufficient stability and durability due to the lack of stable chemical bonding between the coating and the fiber surface. So far, only a few COF coated fibers were prepared by *in situ* hydrothermal growth[48] and covalent bonding approach.[49] However, the reported covalent

[a]State Key Laboratory of Food Science and Technology, Jiangnan University, Wuxi 214122, China. E-mail: xpyan@jiangnan.edu.com

[b]International Joint Laboratory on Food Safety, Jiangnan University, Wuxi 214122, China

[c]Institute of Analytical Food Safety, School of Food Science and Technology, Jiangnan University, Wuxi 214122, China

[d]Key Laboratory of Synthetic and Biological Colloids, Ministry of Education, Jiangnan University, Wuxi 214122, China

† Electronic supplementary information (ESI) available: Additional figures for characterization, solvent stability, and reusability, and additional tables for MS parameters and analytical results. See DOI: 10.1039/c9ta02974e

bonding methods still require reactions under harsh conditions (high temperatures).

Herein, we report room-temperature preparation of a novel COF (named TFPB-BD) from 1,3,5-tris-(4-formylphenyl)benzene (TFPB) and benzidine (BD) and *in situ* room-temperature fabrication of a TFPB-BD bonded stainless steel fiber. The developed TFPB-BD bonded fiber offers high stability and excellent performance for SPME coupled with GC/MS/MS for the determination of trace PCBs in aquatic products.

Experimental section

Chemicals and reagents

All chemical reagents were at least of analytical grade. Wahaha ultrapure water (Wahaha Foods Co. Ltd, Hangzhou, China) was used throughout the experiment. TFPB was purchased from Tongchuangyuan Pharmaceutical Technology Co. Ltd (Chengdu, China). Isooctane, BD, mesitylene, and 3-aminopropyltriethoxysilane (APTES) were obtained from Aladdin Chemistry Co. Ltd (Shanghai, China). A stock standard solution (3 mg L^{-1}) of seven PCBs (28, 52, 101, 118, 138, 153 and 180) in isooctane was obtained from Aladdin Reagent Co. Ltd (Shanghai, China). Acetonitrile (ACN), methanol (MeOH), ethanol (EtOH), *N*,*N*-dimethylformamide (DMF), dichloromethane (DCM), tetrahydrofuran (THF), 1,4-dioxane and acetone were purchased from Sinopharm Chemical Reagent Co. Ltd (Shanghai, China). A series of working standard solutions at various concentrations of PCBs were prepared by gradual dilution of the stock solution with isooctane for further analysis.

Instrumentation

Powder X-ray diffraction (PXRD) patterns were recorded with a D2 PHASER diffractometer (Bruker AXS GmbH, Germany). Fourier transform infrared (FT-IR) spectra were measured on a Nicolet IS20 spectrometer (Nicolet, USA). Thermogravimetric analysis (TGA) was performed on a PTC-10A thermal gravimetric analyzer (Rigaku, Japan). Scanning electron microscope (SEM) images were recorded on a su1510 scanning electron microscope (Rigaku, Japan). Transmission electron microscopy (TEM) images were obtained on a JEM-2100 transmission electron microscope (Rigaku, Japan). N_2 adsorption experiments were performed on an Autosorb-iQ analyzer (Quantachrome, USA).

Identification and quantification of PCBs were performed on a 7890B/7000D GC/MS/MS (Agilent, USA) system fitted with a Rxi-5MS capillary column (30 m × 0.25 mm i.d. × 0.25 μm). The instrumental conditions were as follows: splitless mode; ion source temperature, 230 °C; transfer line temperature, 280 °C; temperature program: the column temperature was initially set at 100 °C, rising to 280 °C at 30 °C min^{-1}, and from 280 °C to 310 °C at 20 °C min^{-1}. The total analysis time was 9 min. Data acquisition was performed in selected multiple reaction monitoring (MRM) mode. Other GC/MS/MS parameters for the determination of PCBs are shown in Table S1 (ESI†). Commercial PDMS (30 μm) and PDMS/DVB (65 μm) coated commercial SPME fibers (Supelco, Bellefonte, USA) were used for comparison.

Room-temperature preparation of TFPB-BD

TFPB (62.5 mg, 0.16 mmol) and BD (44.2 mg, 0.24 mmol) were suspended in a mixture of mesitylene and 1,4-dioxane (1 : 1 v/v, 6 mL) in a 15 mL centrifuge tube, then sonicated for 10 min to obtain a homogeneous dispersion. Subsequently, acetic acid solution (0.6 mL, 6 M) was slowly added to the mixture. The tube was then sealed and left undisturbed at room temperature for 3 d. The yellow precipitate was collected by centrifugation and sequentially washed with THF, DMF, and acetone. The collected powder was dried under vacuum at 120 °C for 12 h to give a yellow TFPB-BD powder with 86.0% isolated yield.

In situ room-temperature fabrication of a TFPB-BD bonded fiber

A stainless steel wire fiber (SS, 23 cm × 0.22 mm) was used as a substrate for the preparation of a SPME fiber. Briefly, one end of SS (3 cm) was immersed in aqua regia for 15 min. Then, the etched part was washed with ultrapure water and dried in air. The dried etched SS was immersed into a mixture of APTES/MeOH/H_2O (v/v/v, 4 : 5 : 1) solution for 4 h and dried in a vacuum oven for 2 h to obtain the amino-functionalized SS fiber (SS-NH_2). The SS-NH_2 fiber was immersed into a solution containing anhydrous dioxane (3 mL), mesitylene (3 mL) and TFPB (62.5 mg, 0.16 mmol) in a centrifuge tube at room temperature for 4 h. Subsequently, BD (44.2 mg, 0.24 mmol) and acetic acid (0.6 mL, 6 M) were added and the reaction continued for 3 d at room temperature. Finally, the TFPB-BD bonded fiber was washed with THF to remove unreacted ligands, and dried in a vacuum oven for 2 h.

Sample preparation

All aquatic products (snakeheads, catfish, bream, crucian, white shrimp and base shrimp) were collected from local markets. The muscles of the aquatic products were chopped and homogenized with a blender. Then, 1.0 g of the homogenized sample was weighed and extracted with a solvent mixture of *n*-hexane and acetone (10 mL, 1 : 1 v/v) under ultrasound irradiation for 30 min. The supernatant was collected by centrifugation at 8000 rpm for 10 min and the sediment was extracted repeatedly. Then, all supernatants were combined and dried with N_2 gas at ambient temperature and the residues were dissolved with 1.0 mL of isooctane for further use.

SPME procedures

All extractions were performed in headspace SPME (HS-SPME) mode. Working solutions of the PCBs were prepared for SPME by diluting 10 μL of sample solution or working standard solution to 10 mL with ultrapure water. SPME was performed in a Teflon-lined 20 mL glass vial. The needle of the SPME device was passed through the septum, and the SPME fiber was exposed to the headspace of the working solution at 70 °C for 50 min under magnetic stirring at 1000 rpm. After extraction, the fiber was removed from the vial and immediately inserted into the GC inlet for thermal desorption at 300 °C for 5 min and

subsequent GC/MS/MS analysis. Before each extraction, the fiber was conditioned at 310 °C for 30 min.

Results and discussion

Room-temperature preparation and characterization of TFPB-BD

COFs were typically prepared under harsh conditions such as high temperature and pressure, which are not favorable for the *in situ* preparation of COF bonded SPME fiber. Here, we show room-temperature fabrication of a new COF TFPB-BD (Fig. 1a). The new imine-linked COF TFPB-BD was successfully synthesized *via* condensation of BD with TFPB at room temperature.

To determine the crystal structure of the TFPB-BD, PXRD experiments and Pawley refinements were conducted. The PXRD pattern of TFPB-BD shows several peaks at 2.31°, 4.03° and 6.10°, which agreed well with that of the simulated structure of TFPB-BD produced with eclipsed AA stacking mode with unit cell parameters $a = b = 43.7789$ Å, $c = 4.0603$ Å, $\alpha = \beta = 90°$ and $\gamma = 120°$ (Fig. 2a; Table S2, ESI†). The refined PXRD pattern well reproduces the experimental PXRD pattern with factors of $R_{wp} = 9.22\%$ and $R_p = 6.30\%$ (Fig. S1, ESI†). The FT-IR spectra of TFPB-BD demonstrate a typical C=N stretching band at 1618 cm^{-1}. The C=O peak (1686 cm^{-1}) of the TFPB was strongly attenuated and the N–H stretching peaks (3300–3400 cm^{-1}) of BD disappeared (Fig. 2b). These results indicate the successful condensation of TFPB and BD with imine-linked bonds. The as-prepared TFPB-BD has a Brunauer–Emmett–Teller (BET) surface area of 286 $m^2 g^{-1}$ and a pore size of *ca.* 32 Å (Fig. 2c and d). The as-synthesized TFPB-BD showed globular particles with a size of *ca.* 1.2 μm (Fig. S2 and S3, ESI†). The as-prepared TFPB-BD is not only thermally stable up to 430 °C (Fig. S4†), but also chemically stable in conventional solvents such as water, ACN, EtOH, DCM and THF (Fig. S5 and S6, ESI†).

In situ room-temperature fabrication and characterization of the TFPB-BD bonded fiber

The successful room-temperature synthesis of COF TFPB-BD prompted us to explore the possibility for *in situ* room-temperature fabrication of the COF bonded SPME fiber. As shown in Fig. 1b, the etched SS was modified with APTES to provide the amino groups for subsequent reaction with the aldehyde groups on TFPB for *in situ* room-temperature fabrication of the TFPB-BD bonded fiber.

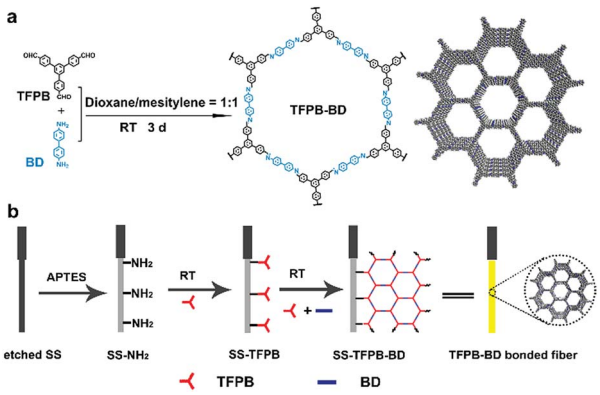

Fig. 1 (a) Illustration of room-temperature synthesis of TFPB-BD *via* the condensation of TFPB and BD. Graphic view of TFPB-BD for the 2D eclipsed model (gray, C; blue, N; H is omitted for clarity). (b) Schematic of *in situ* room-temperature preparation of the TFPB-BD bonded fiber.

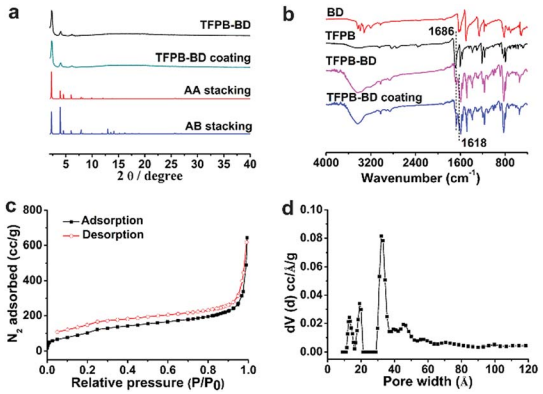

Fig. 2 (a) Comparison of the PXRD patterns of the as-synthesized TFPB-BD (black), the TFPB-BD scraped from the SPME fibers (dark cyan) with a simulated pattern for the AA eclipsed model (red) and the AB staggered model (blue). (b) FT-IR spectra of BD (red), TFPB (black), the as-synthesized TFPB-BD (magenta) and TFPB-BD scraped from the SPME fibers (blue). (c) N_2 adsorption–desorption isotherms of the as-prepared TFPB-BD. (d) Pore size distribution of the as-synthesized TFPB-BD.

The interaction between the COF layers and the fiber was revealed by comparing the FT-IR spectra of SS-NH_2 and SS-TFPB (Fig. S7, ESI†). The presence of Si–O (1134 cm^{-1}) and N–H stretching peaks (3300–3400 cm^{-1}) in the FT-IR spectra of SS-NH_2 indicate the successful modification of APTES. The appearance of C=N (1643 cm^{-1}) and C=O (1686 cm^{-1}) and the disappearance of N–H stretching peaks (3300–3400 cm^{-1}) indicate successful TFPB functionalization on the SS-NH_2 fiber. In addition, a typical C=N stretching band at 1618 cm^{-1} further demonstrates the growth of the COF TFPB-BD on the SS-TFPB fiber. The PXRD patterns, FT-IR spectra and TEM images of the TFPB-BD coating scraped from the prepared SPME fiber were comparable with those of the as-prepared TFPB-BD (Fig. 2a, b and 3d), showing the successful growth of TFPB-BD coating on the SS fiber. SEM images show the presence of a uniform spherical COF coating on the surface of SS fibers, and the thickness of the coating is about 10 μm (Fig. 3).

Application of the TFPB-BD bonded fiber for SPME of PCBs

We applied TFPB-BD bonded fibers to subsequent SPME experiments to demonstrate their enrichment capability for PCBs. Potential parameters affecting the extraction performance of PCBs on the TFPB-BD bonded fiber, such as extraction temperature and time, and desorption temperature and time, were optimized (Fig. 4).

Extraction temperature has great effects on SPME due to its influence on the analyte concentration in the headspace and adsorption process. High temperature is favorable for the transfer of analytes from aqueous solution to the headspace,

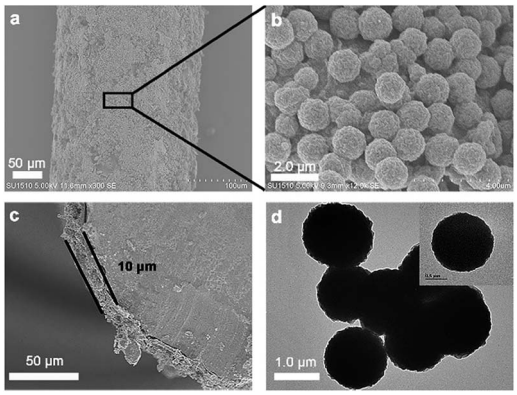

Fig. 3 SEM images of the TFPB-BD bonded fiber with magnification at (a) 300× and (b) 12 000×; (c) SEM image of the cross section of the TFPB-BD bonded fiber; (d) TEM image of TFPB-BD scraped from the SPME fibers.

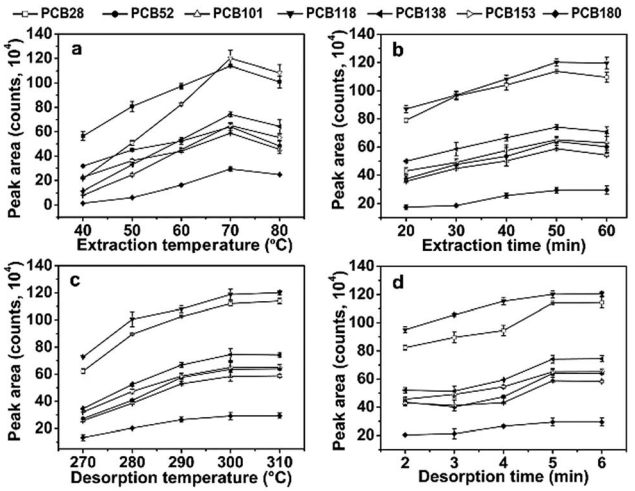

Fig. 4 Effects of experimental conditions on the extraction efficiency of the TFPB-BD bonded fiber for 100 ng L^{-1} PCBs: (a) extraction temperature (extraction for 50 min, desorption at 300 °C for 5 min); (b) extraction time (extraction at 70 °C, desorption at 300 °C for 5 min); (c) desorption temperature (extraction at 70 °C for 50 min, desorption for 5 min); (d) desorption time (extraction at 70 °C for 50 min, desorption at 300 °C).

but is unfavorable for the exothermic adsorption of the gaseous analytes on the SPME fiber. Fig. 4a shows the effect of extraction temperature on the extraction efficiency. The peak areas of PCBs increased steadily with extraction temperature from 40 °C to 70 °C, and then decreased with a further increase of temperature to 80 °C. Therefore, 70 °C was used for subsequent experiments.

SPME needs sufficient time to reach the extraction equilibrium, so we tested the effect of the extraction time on the SPME of PCBs. As shown in Fig. 4b, the peak areas of PCBs increased with extraction time up to 50 min, and then remained unchanged with further increase of extraction time. To achieve the best extraction efficiency for PCBs, 50 min was chosen for SPME.

The effects of desorption temperature and time were also examined to ensure the complete release of the adsorbed analytes from the SPME fiber. It was found that a desorption temperature of 300 °C with a desorption time of 5 min were sufficient for quantitative desorption of the analytes (Fig. 4c and d).

Comparison of different SPME fibers

To investigate the extraction performance of TFPB-BD for PCBs, additional SPME experiments for PCBs were conducted on the commercial PDMS (30 μm) coated fiber, PDMS/DVB (65 μm) coated fiber and bare-etched SS fiber (Fig. 5). For comparison, enhancement factor (EF) was determined as the ratio of the sensitivity of the analyte after extraction to that before extraction (*i.e.* by direct injection of 1 μL standard solution) using the chromatographic peak area for quantification.[9] The TFPB-BD bonded fiber gave much larger EFs than the bare-etched SS fiber, demonstrating the excellent extraction performance of the TFPB-BD coating for PCBs. Compared to the other two commercial fibers, the TFPB-BD bonded fiber also offered significantly larger EFs for PCBs even if the TFPB-BD coating is much thinner. The larger EFs of the TFPB-BD bonded fiber for PCBs resulted from hydrophobicity,[21,43,44,50] π–π stacking interaction[42–44,48,49] and steric hindrance effects[45,50] between TFPB-BD and PCBs. These π–π and hydrophobic interactions between analytes and the aromatic frameworks of the TFPB-BD also make the TFPB-BD bonded fibers suitable for other aromatic toxic organic pollutants.

Analytical figures of merit

The analytical performance of the TFPB-BD bonded fiber for the SPME of PCBs is summarized in Table 1. The EFs for PCBs ranged from 4471 to 7488. The detection limits (LODs) (S/N = 3) and quantification limits (LOQs) (S/N = 10) of the TFPB-BD bonded SPME fiber for the PCBs ranged from 0.07 μg L^{-1} to 0.35 μg L^{-1} and from 0.24 μg L^{-1} to 1.17 μg L^{-1}, respectively. The relative standard deviation (RSD) of the peak areas obtained

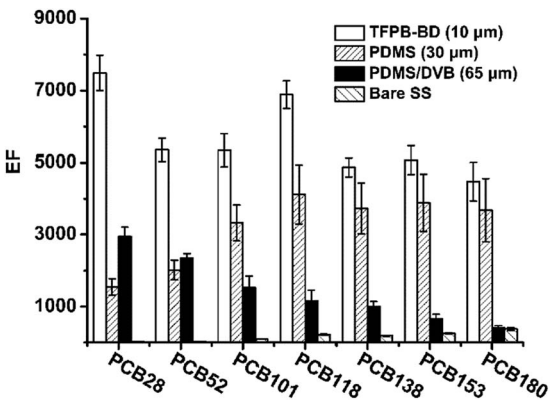

Fig. 5 Comparison of the TFPB-BD bonded fiber, commercial PDMS coated fiber, commercial PDMS/DVB coated fiber and etched SS fiber for SPME of 50 ng L^{-1} PCBs (extraction at 70 °C for 50 min; desorption at 300 °C for 5 min; for commercial fibers, the desorption temperature was 270 °C due to the recommended maximum service temperature of 270 °C).

Table 1 Analytical performance of the TFPB-BD bonded fiber for the SPME of PCBs

Analyte	Linear range (ng L^{-1})	r^2	LODs (ng L^{-1}, S/N = 3)	LOQs (ng L^{-1}, S/N = 10)	RSD		EFs
					One fiber (%, $n = 6$)	Fiber to fiber (%, $n = 3$)	
PCB28	1–1000	0.9999	0.08	0.26	5.0	5.3	7488
PCB52	1–500	0.9998	0.10	0.32	3.8	5.3	5358
PCB101	3–500	0.9998	0.12	0.40	5.8	8.2	5342
PCB118	1–1000	0.9984	0.07	0.24	8.3	8.5	6888
PCB138	1–500	0.9995	0.11	0.36	5.7	7.6	4869
PCB153	1–500	0.9990	0.13	0.44	7.8	9.8	5072
PCB180	3–1000	0.9969	0.35	1.17	8.8	9.7	4471

from six replicate extractions of PCB working standard solutions was from 3.8% to 8.8%. The RSD of the peak areas obtained from three parallel prepared fibers was from 5.3% to 9.8%. In addition, the peak areas of 100 ng L^{-1} PCBs show no significant change after 180 extraction cycles with the same TFPB-BD bonded fiber (Fig. S8, ESI†). Comparison of our method with previous SPME methods for PCBs based on other sorbents such as CuO nanosheets,[18] ZnO nanoflakes,[19] MoS_2/RGO,[20] MOFs[21,22] and polymeric ionic liquid[24] shows that our method possesses relatively lower LODs, better or comparable precision for PCBs (Table 2), indicating the great potential of COF-based SPME in sample pretreatment.

Application to the analysis of aquatic products

The developed method was applied to the analysis of aquatic products including snakeheads, catfish, bream, crucian, white shrimp and base shrimp for PCBs. The analytical results are shown in Table S3 (ESI†). All the PCBs in the base shrimp samples were below the LODs or LOQs. However, the PCBs were detected in all other aquatic products including snakehead, catfish, bream, crucian and white shrimp samples with a maximum concentration of 1.5 μg kg^{-1}. The accuracy of the developed method was demonstrated by a recovery study with spiking 1.0 μg kg^{-1} PCBs in the aquatic products. The recoveries obtained ranged from 87.1% to 99.7%. The results show the feasibility of the developed method for the determination of PCBs in aquatic products. Fig. 6 shows the GC/MS/MS chromatograms for PCBs in a standard solution and real samples after SPME using the TFPB-BD bonded fiber.

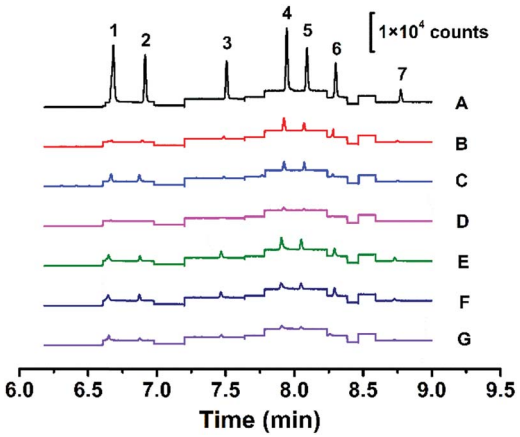

Fig. 6 GC/MS/MS chromatograms of PCBs after SPME using the TFPB-BD bonded fiber: (A) 3 ng L^{-1} standard solution of PCBs; (B) catfish sample; (C) snakehead sample; (D) base shrimp sample; (E) crucian sample; (F) bream sample; (G) white shrimp sample. Peak identity: (1) PCB28; (2) PCB52; (3) PCB101; (4) PCB118; (5) PCB138; (6) PCB153; (7) PCB180.

Table 2 Comparison with other reported methods for the determination of PCBs

Method	Coating	LODs (ng L^{-1})	RSDs (%)	Ref.
GC/MS	MIL-88B	0.45–1.32	4.2–8.7	21
GC/MS	MOF-177	0.69–4.42	1.5–8.7	22
GC/MS	MoS_2/RGO[a]	51–93	—	20
HPLC-UV	ZnONFs[b]	20–170	5.5–11	19
HPLC-UV	CuO nanosheet	25–50	5.2–8.6	18
GC-ECD	Poly-IL[c]	0.9–5.8	3.0–11	24
GC/MS/MS	TFPB-BD	0.08–0.35	3.8–8.8	Our work

[a] RGO, reduced graphene oxide. [b] ZnONFs, ZnO nanoflakes. [c] Poly-IL, polymeric ionic liquid.

Conclusions

In conclusion, we have reported room-temperature fabrication of a new COF TFPB-BD as SPME coating and a simple *in situ* room-temperature method for the fabrication of uniform TFPB-BD bonded SPME fibers. The prepared novel TFPB-BD bonded fibers offer high thermal and chemical stability and excellent reusability. We have also applied the prepared TFPB-BD bonded fibers for SPME of PCBs in aquatic products before GC/MS/MS determination with high enhancement factors, low detection limits, excellent reproducibility and accuracy. Further work will extend the application of the TFPB-BD bonded fibers for the extraction of other aromatic toxic organic pollutants in environmental and food samples.

Conflicts of interest

There are no conflicts to declare.

Acknowledgements

This work was supported by the National Natural Science Foundation of China (No. 21775056), National Basic Research Program of China (No. 2015CB932001), China Postdoctoral Science Foundation (No. 2018M630510), Fundamental Research Funds for the Central Universities (No. JUSRP51714B), and National First-class Discipline Program of Food Science and Technology (No. JUFSTR20180301).

Notes and references

1 S. H. Safe, *Crit. Rev. Toxicol.*, 1994, **24**, 87–149.
2 E. Silva, M. Mascini, S. Centi and A. P. F. Turner, *Anal. Lett.*, 2007, **40**, 1371–1385.
3 C. L. Arthur and J. Pawliszyn, *Anal. Chem.*, 1990, **62**, 2145–2148.
4 H.-L. Xu, Y. Li, D.-Q. Jiang and X.-P. Yan, *Anal. Chem.*, 2009, **81**, 4971–4977.
5 É. A. Souza-Silva, E. Gionfriddo and J. Pawliszyn, *Trends Anal. Chem.*, 2015, **71**, 236–248.
6 J. J. Poole, J. J. Grandy, M. Yu, E. Boyaci, G. A. Gómez-Ríos, N. Reyes-Garcés, B. Bojko, H. V. Heide and J. Pawliszyn, *Anal. Chem.*, 2017, **89**, 8021–8026.
7 G. A. Gómez-Ríos, E. Gionfriddo, J. Poole and J. Pawliszyn, *Anal. Chem.*, 2017, **89**, 7240–7248.
8 M. N. A. Khalil, M. I. Fekry and M. A. Farag, *Food Chem.*, 2017, **217**, 171–181.
9 X.-Y. Cui, Z.-Y. Gu, D.-Q. Jiang, Y. Li, H.-F. Wang and X.-P. Yan, *Anal. Chem.*, 2009, **81**, 9771–9777.
10 Y.-A. Li, F. Yang, Z.-C. Liu, Q.-K. Liu and Y.-B. Dong, *J. Mater. Chem. A*, 2014, **2**, 13868–13872.
11 L. K. Wee, N. Janssens, J. Vercammen, L. Tamaraschi, L. C. J. Thomassen and J. A. Martens, *J. Mater. Chem. A*, 2015, **3**, 2258–2264.
12 O. Nacham, K. D. Clark and J. L. Anderson, *Anal. Chem.*, 2016, **88**, 7813–7820.
13 O. Nacham, K. D. Clark, M. Varona and J. L. Anderson, *Anal. Chem.*, 2017, **89**, 10661–10666.
14 M. Varona, X. Ding, K. D. Clark and J. L. Anderson, *Anal. Chem.*, 2018, **90**, 6922–6928.
15 Y. Chen, S. T. J. Droge and J. L. M. Hermens, *J. Chromatogr. A*, 2012, **1252**, 15–22.
16 A. Derouiche, M. R. Driss, J.-P. Morizur and M.-H. Taphanel, *J. Chromatogr. A*, 2007, **1138**, 231–243.
17 M. Polo, M. Llompart, C. Garcia-Jares, G. Gomez-Noya, M.-H. Bollain and R. Cela, *J. Chromatogr. A*, 2006, **1124**, 11–21.
18 Y. X. Yang, Y. Lei, R. Zhang, X. M. Wang and X. Z. Du, *Anal. Methods*, 2018, **10**, 4044–4052.
19 J. J. Du, H. J. Wang, R. Zhang, X. M. Wang, X. Z. Du and X. Q. Lu, *Microchim. Acta*, 2018, **185**, 441–449.
20 F. Y. Lv, N. Gan, Y. T. Cao, Y. Zhou, R. J. Zuo and Y. R. Dong, *J. Chromatogr. A*, 2017, **1525**, 42–50.
21 Y.-Y. Wu, C.-X. Yang and X.-P. Yan, *J. Chromatogr. A*, 2014, **1334**, 1–8.
22 G. H. Wang, Y. Q. Lei and H. C. Song, *Talanta*, 2015, **144**, 369–374.
23 N. Zhang, C. H. Huang, Z. M. Feng, H. Chen, P. Tong, X. P. Wu and L. Zhang, *J. Chromatogr. A*, 2018, **1570**, 10–18.
24 J. Li, F. Q. Wang, J.-F. Wu and G.-C. Zhao, *Microchim. Acta*, 2017, **184**, 2621–2628.
25 A. P. Côté, A. I. Benin, N. W. Ockwig, M. O'Keeffe, A. J. Matzger and O. M. Yaghi, *Science*, 2005, **310**, 1166–1170.
26 H. M. El-Kaderi, J. R. Hunt, J. L. Mendoza-Cortés, A. P. Côté, R. E. Taylor, M. O'Keeffe and O. M. Yaghi, *Science*, 2007, **316**, 268–272.
27 H. Furukawa and O. M. Yaghi, *J. Am. Chem. Soc.*, 2009, **131**, 8875–8883.
28 M. G. Rabbani, A. K. Sekizkardes, Z. Kahveci, T. E. Reich, R. S. Ding and H. M. El-Kaderi, *Chem.–Eur. J.*, 2013, **19**, 3324–3328.
29 N. Huang, X. Chen, R. Krishna and D. L. Jiang, *Angew. Chem., Int. Ed.*, 2015, **54**, 2986–2990.
30 H. Li, Q. Y. Pan, Y. C. Ma, X. Y. Guan, M. Xue, Q. R. Fang, Y. S. Yan, V. Valtchev and S. L. Qiu, *J. Am. Chem. Soc.*, 2016, **138**, 14783–14788.
31 X. R. Wang, X. Han, J. Zhang, X. W. Wu, Y. Liu and Y. Cui, *J. Am. Chem. Soc.*, 2016, **138**, 12332–12335.
32 J. Zhang, X. Han, X. W. Wu, Y. Liu and Y. Cui, *J. Am. Chem. Soc.*, 2017, **139**, 8277–8285.
33 Z. P. Li, Y. W. Zhang, H. Xia, Y. Mu and X. M. Liu, *Chem. Commun.*, 2016, **52**, 6613–6616.
34 H.-L. Qian, C. Dai, C.-X. Yang and X.-P. Yan, *ACS Appl. Mater. Interfaces*, 2017, **9**, 24999–25005.
35 Q. Gao, X. Li, G.-H. Ning, K. Leng, B. B. Tian, C. B. Liu, W. Tang, H.-S. Xu and K. P. Loh, *Chem. Commun.*, 2018, **54**, 2349–2352.
36 B. P. Biswal, S. Kandambeth, S. Chandra, D. B. Shinde, S. Bera, S. Karak, B. Garai, U. K. Kharul and R. Banerjee, *J. Mater. Chem. A*, 2015, **3**, 23664–23669.
37 Y. Li, C.-X. Yang and X.-P. Yan, *Chem. Commun.*, 2017, **53**, 2511–2514.
38 A. Mellah, S. P. S. Fernandes, R. Rodríguez, J. Otero, J. Paz, J. Cruces, D. D. Medina, H. Djamila, B. Espiña and L. M. Salonen, *Chem.–Eur. J.*, 2018, **24**, 1–6.
39 H.-L. Qian, C.-X. Yang and X.-P. Yan, *Nat. Commun.*, 2016, **7**, 12104.
40 C. H. Liu, E. Park, Y. H. Jin, J. Liu, Y. X. Yu, W. Zhang, S. B. Lei and W. P. Hu, *Angew. Chem., Int. Ed.*, 2018, **57**, 8984–8988.
41 C.-X. Yang, C. Liu, Y.-M. Cao and X.-P. Yan, *Chem. Commun.*, 2015, **51**, 12254–12257.
42 S. H. Zhang, Q. Yang, Z. Li, W. C. Wang, C. Wang and Z. Wang, *Anal. Bioanal. Chem.*, 2017, **409**, 3429–3439.
43 T. Wu, X. H. Zang, M. T. Wang, Q. Y. Chang, C. Wang, Q. H. Wu and Z. Wang, *J. Agric. Food Chem.*, 2018, **66**, 11158–11165.
44 L. Liu, W.-K. Meng, Y.-S. Zhou, X. Wang, G.-J. Xu, M.-L. Wang, J.-M. Lin and R.-S. Zhao, *Chem. Eng. J.*, 2019, **356**, 926–933.

45 M. T. Wang, X. Zhou, X. H. Zang, Y. C. Pang, Q. Y. Chang, C. Wang and Z. Wang, *J. Sep. Sci.*, 2018, **41**, 4038–4046.
46 W. Gao, Y. Tian, H. Liu, Y. Q. Cai, A. F. Liu, Y.-L. Yu, Z. S. Zhao and G. B. Jiang, *Anal. Chem.*, 2019, **91**, 772–775.
47 X. M. Yang, J. M. Wang, W. J. Wang, S. H. Zhang, C. Wang, J. H. Zhou and Z. Wang, *Microchim. Acta*, 2019, **186**, 145.
48 M. X. Wu, G. Chen, P. Liu, W. H. Zhou and Q. Jia, *J. Chromatogr. A*, 2016, **1456**, 34–41.
49 M. X. Wu, G. Chen, J. T. Ma, P. Liu and Q. Jia, *Talanta*, 2016, **161**, 350–358.
50 Q.-L. Li, X. Wang, Y.-L. Liu, X.-F. Chen, M.-L. Wang and R.-S. Zhao, *J. Chromatogr. A*, 2014, **1374**, 58–65.